

Numerics Exercise 2

Anthony Tran

November 2025

1 1



Figure 1: Sketch of rectangular cross-section.

For a rectangular cross section, the area is given by:

$$A = w_0 \times h \quad (1)$$

Rearranging the expression, we find that:

$$h = \frac{A}{w_0}$$

The wetted parts of the rectangular geometry will only be made of the base, w_0 , and the two heights, $2h$.

Hence, the perimeter will be given by:

$$w_0 + 2h = w_0 + 2\frac{A}{w_0}$$

We are given the equation:

$$\frac{\partial A}{\partial t} + \frac{\partial F(A, s)}{\partial s} = 0 \quad (2)$$

with

$$F(A, s) = \frac{A^{5/3}\sqrt{-\partial_s b}}{C_m P(A, s)^{2/3}}$$

To simplify the equation, we note that:

$$P(A, s) = w_0(s) + 2A/(w_0(s))$$

Hence, we may rewrite $F(A, s)$ as:

$$\begin{aligned} F(A, s) &= \frac{A^{5/3}\sqrt{-\partial_s b}}{C_m(w_0(s) + 2A/(w_0(s)))^{2/3}} \\ \frac{\partial F}{\partial s} &= \frac{\partial F}{\partial A} \frac{\partial A}{\partial s} + \frac{\partial F}{\partial s} \end{aligned} \quad (3)$$

We apply the quotient rule:

$$\frac{d}{dx} \left(\frac{u(x)}{v(x)} \right) = \frac{u'(x)v(x) - u(x)v'(x)}{[v(x)]^2}$$

$$\frac{\partial F}{\partial A} = \frac{5A^{2/3}\sqrt{-\partial_s b}C_m(w_0(s) + 2A/(w_0(s)))^{2/3}}{3C_m^2(w_0(s) + 2A/(w_0(s)))^{4/3}} - \frac{2C_m A^{5/3}\sqrt{-\partial_s b}(2/w_0)(w_0 + 2A/(w_0))^{-1/3}}{3C_m^2((w_0(s) + 2A/(w_0(s)))^{4/3})} \quad (4)$$

We can simplify this:

$$\frac{\partial F}{\partial A} = \frac{5A^{2/3}\sqrt{-\partial_s b}}{3C_m(w_0(s) + 2A/(w_0(s)))^{2/3}} - \frac{2A^{5/3}\sqrt{-\partial_s b}(2/w_0)}{3C_m((w_0(s) + 2A/(w_0(s)))^{5/3})} \quad (5)$$

$$\frac{\partial F}{\partial A} = \frac{5A^{2/3}\sqrt{-\partial_s b}}{3C_m(w_0(s) + 2A/(w_0(s)))^{2/3}} - \frac{4A^{5/3}\sqrt{-\partial_s b}}{3C_m((w_0(s) + 2A/(w_0(s)))^{5/3})w_0} \quad (6)$$

$$\frac{\partial F}{\partial A} = \frac{5A^{2/3}\sqrt{-\partial_s b}w_0(w_0 + 2A/w_0)}{3C_m(w_0(s) + 2A/(w_0(s)))^{5/3}w_0} - \frac{4A^{5/3}\sqrt{-\partial_s b}}{3C_m((w_0(s) + 2A/(w_0(s)))^{5/3})w_0} \quad (7)$$

$$\frac{\partial F}{\partial A} = \frac{\sqrt{-\partial_s b}}{3C_m} \frac{5A^{2/3}w_0 + (6A^{5/3}/w_0)}{(w_0 + 2A/w_0)^{5/3}} \quad (8)$$

To find $\frac{\partial F}{\partial s}$ we find:

$$\begin{aligned} \frac{\partial F}{\partial s} &= \frac{\partial F}{\partial w_0} \frac{\partial w_0}{\partial s} \\ \frac{\partial F}{\partial s} &= -A^{5/3}\sqrt{-\partial_s b} \frac{2(w_0 + 2A/(w_0))^{-5/3}}{3C_m} \left(\frac{dw_0}{ds} - 2A(w_0)^{-2} \frac{dw_0}{ds} \right) \end{aligned} \quad (9)$$

$$\frac{\partial F}{\partial s} = -\frac{2A^{5/3}\sqrt{-\partial_s b}}{3C_m(w_0 + 2A/(w_0))^{5/3}} \left(1 - \frac{2A}{w_0^2} \right) \frac{dw_0}{ds} \quad (10)$$

1.1 2

In the limit where w_0 is independent of s , we find that :

$$\frac{\partial F}{\partial s} = 0$$

Hence, the equation reduces to a quasi-linear PDE:

$$\frac{\partial A}{\partial t} + \frac{\partial F}{\partial A} \frac{\partial A}{\partial s} = 0 \quad (11)$$

with $\lambda = \partial_A F$ being the "eigenvalue.

For the Riemann problem, we define the initial condition:

$$A(s, 0) = \begin{cases} A_L = A_j & s < 0, \\ A_R = A_{j+1} & s > 0. \end{cases} \quad (12)$$

In this problem, s is given by:

$$s = s_0 + \lambda t \quad (13)$$

Hence, if we know the initial position, we know s , i.e

$$s - \lambda t = s_0 \quad (14)$$

Therefore, we can say:

$$A(s_0, t = 0) = A(s - \lambda t, t = 0) \quad (15)$$

Therefore, the solution to our Riemann problem is:

$$A(s - at, 0) = \begin{cases} A_L = A_j & s < \lambda t, \\ A_R = A_{j+1} & s > \lambda t. \end{cases} \quad (16)$$

We can have either a shock or a rarefaction as the solution:

When we have a shock, we have $A_L > A_R$.

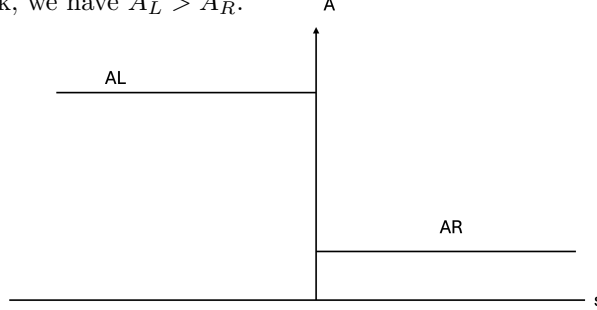


Figure 2: Sketch of initial condition for shock.

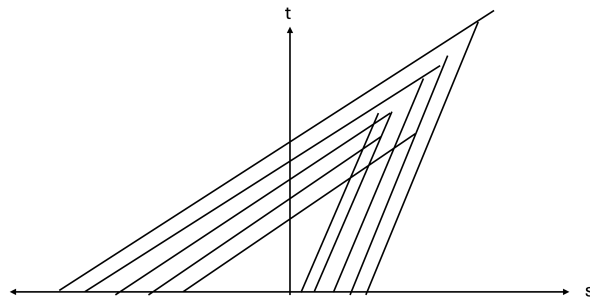


Figure 3: Sketch of characteristics.

The shock speed, σ , of the shock is given by the Rankine-Hugoniot equation:

$$\sigma = \frac{F(A_R) - F(A_L)}{A_R - A_L} \quad (17)$$

The solution to the problem in this case is:

$$A(s - at, 0) = \begin{cases} A_L = A_j & s < \sigma t, \\ A_R = A_{j+1} & s > \sigma t. \end{cases} \quad (18)$$

The second case is the rarefaction with $A_L < A_R$

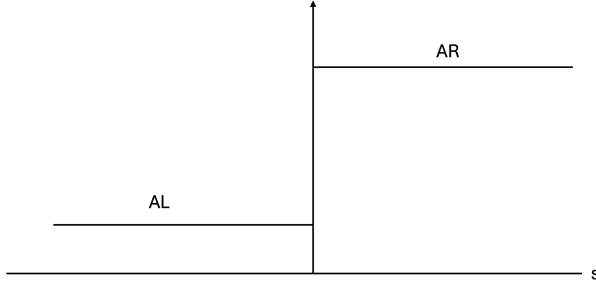


Figure 4: Sketch of initial condition for rarefaction.

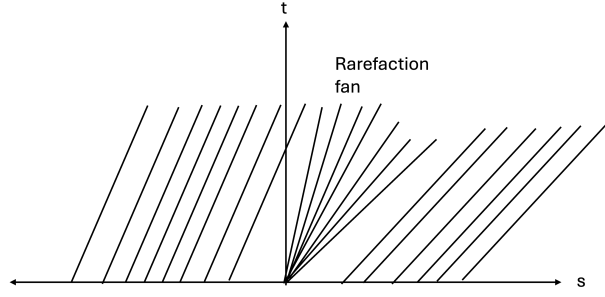


Figure 5: Sketch of initial condition for rarefaction.

In this particular case, we can derive a similarity solution where A is a function of $\eta = \frac{s}{t}$. Applying the chain-rule to the conservation law gives:

$$-A'(\eta)\left(\frac{s}{t^2}\right) + F'(A)A'(\eta)\frac{1}{t} = 0 \quad (19)$$

$$A'(\eta)\left(-\frac{s}{t^2} + F'(A)\frac{1}{t}\right) = 0 \quad (20)$$

$$A'(\eta)(-\eta + F'(A)) = 0 \quad (21)$$

We clearly have two cases:

if $A'(\eta) = 0$, A is constant and this corresponds to either A_L or A_R . If $-\eta + F'(A) = 0$, we simply find that:

$$\frac{s}{t} = F'(A) = \lambda$$

Hence, we have a fan of straight lines between A_L and A_R . From these conditions and the previous solutions, we find the following solution:

$$A(s - at, 0) = \begin{cases} A_L, & s < \lambda(A_L)t, \\ \lambda^{-1}(\eta), & \lambda(A_L)t \leq s \leq \lambda(A_R)t \\ A_R, & s > \lambda(A_R)t \end{cases} \quad (22)$$

1.2 3

We will start by considering the equation:

$$\frac{\partial A}{\partial t} + \lambda \frac{\partial A}{\partial s} = 0 \quad (23)$$

We can rewrite it in conservation form to give:

$$\frac{\partial A}{\partial t} + \frac{\partial F(A)}{\partial s} = 0 \quad (24)$$

To derive the Godunov scheme, we integrate the above equation in space and time:

$$\int_{s_{-1/2}}^{s+1/2} \int_{t_n}^{t_{n+1}} \frac{\partial A}{\partial t} dt ds + \int_{t_n}^{t_{n+1}} \int_{s_{-1/2}}^{s+1/2} \frac{\partial F(A)}{\partial s} ds dt = 0 \quad (25)$$

$$\int_{s_{-1/2}}^{s+1/2} A(s, t_{n+1}) - A(s, t_n) ds + \int_{t_n}^{t_{n+1}} F(A(s_{+1/2}, t)) - F(A(s_{-1/2}, t)) dt = 0 \quad (26)$$

We now define the cell average:

$$A_k(t) = \frac{1}{h_k} \int_{s_{-1/2}}^{s+1/2} A(s, t) ds \quad (27)$$

where

$$h_k = s_{k+1/2} - s_{k-1/2}$$

We then obtain:

$$A_k^{n+1} = A_k^n - \frac{1}{h_k} \int_{t_n}^{t_{n+1}} F_{k+1/2}(t) - F_{k-1/2}(t) dt \quad (28)$$

where

$$F_{k+1/2}(t) = F(A(s_{+1/2}, t))$$

We can approximate the numerical flux function as:

$$F_{k+1/2}(A_k^n, A_{k+1}^n) = \frac{1}{\Delta t} \int_{t_n}^{t_{n+1}} F_{k+1/2}(t) \quad (29)$$

Substituting this into our equation in the previous question, we find:

$$A_k^{n+1} = A_k^n - \frac{\Delta t}{h_k} (F_{k+1/2}(A_k^n, A_{k+1}^n) - F_{k-1/2}(A_{k-1}^n, A_k^n)) \quad (30)$$

1.3 4

We need to evaluate the flux :

$$F_{k+1/2}(A_k^n, A_{k+1}^n) = \frac{1}{\Delta t} \int_{t_n}^{t_{n+1}} F_{k+1/2}(t) = \frac{1}{\Delta t} \int_{t_n}^{t_{n+1}} F(A(s_{+1/2}, t)) \quad (31)$$

Given that $A(s, t)$ will be constant along the characteristics and that λ is positive, we find that

$$F_{k+1/2}(A_k^n, A_{k+1}^n) = \frac{1}{\Delta t} \int_{t_n}^{t_{n+1}} F(A(s_k^n)) = \lambda A_k^n \quad (32)$$

From our solution in the previous question, we know that the flux goes from the left to the right. Hence, the flux will be upwind.

$$A_k^{n+1} = A_k^n - \lambda \frac{\Delta t}{h_k} (A_k^n - A_{k-1}^n) \quad (33)$$

1.4 5

To find the CFL condition, we make use of the maximum principle again.

We can factorize the equation in the previous question to get:

$$A_k^{n+1} = (1 - \frac{\Delta t}{h_k} \lambda) A_k^n + \frac{\Delta t}{h_k} \lambda A_{k-1}^n \quad (34)$$

The requirement is that :

$$1 - \frac{\Delta t}{h_k} \lambda \geq 0$$

$$\frac{\Delta t}{h_k} \lambda \leq 1$$

Hence,

$$\Delta t \leq \frac{h_k}{|\lambda|}$$

Here, our eigenvalue is $\frac{\partial F}{\partial A}$ is the local wave speed.

Hence, we may rewrite the condition as :

$$\Delta t \leq \frac{h_k 3 C_m}{\sqrt{-\partial_s b}} \frac{(w_0 + 2A_k/w_0)^{5/3}}{(5w_0 A_k^{2/3} + 6A_k^{5/3}/w_0)}$$

1.5 Question 6

At the ghost cell , A_{-1}^n , we need a constant value, i.e A_{in} , given that our flow moves from the left to the right with positive λ . Similarly, at the outlet, we find that we need to set the ghost cell, A_k , to the value of the adjacent cell. Hence, $A_k = A_{k-1}$.

1.6 Question 7

1.6.1 Test Case 0

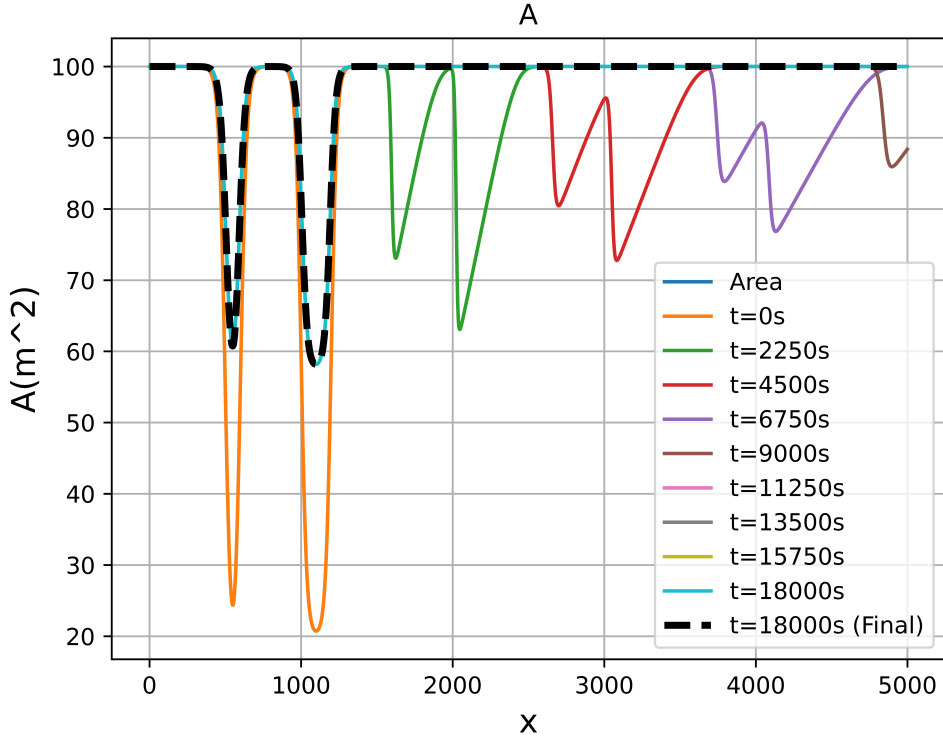


Figure 6: Area at different times

As we can see in Figure 9, the error goes down linearly as we double the grid size. In Figure 10, we see that the error goes up linearly as we increase the time step. Hence, the scheme is first-order accurate in both space and time.

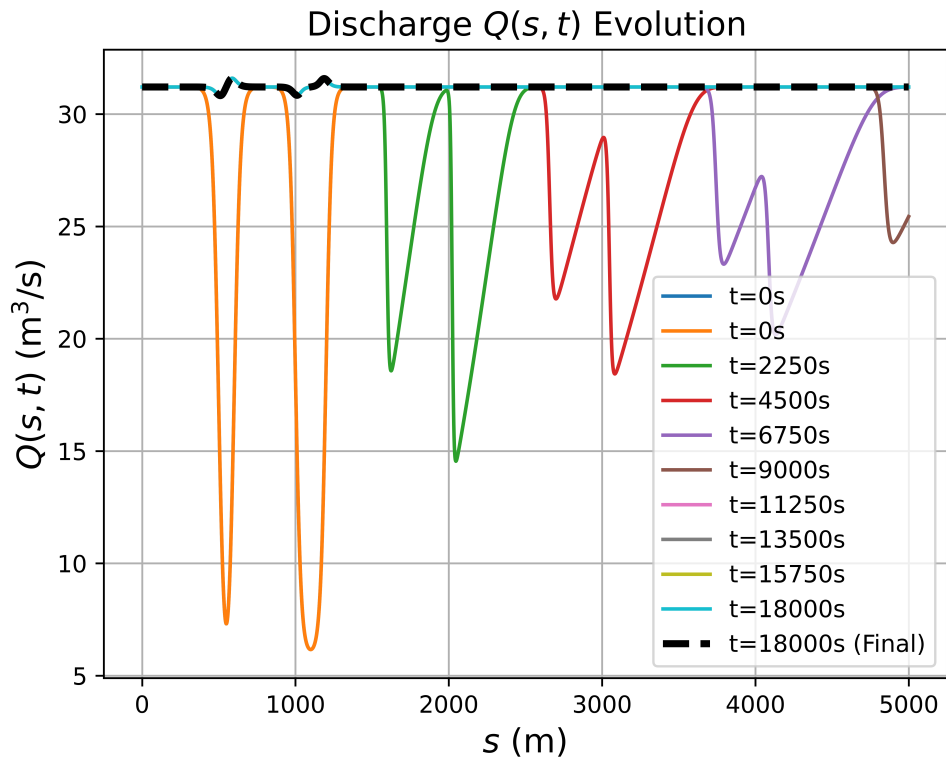


Figure 7: Flux at different times

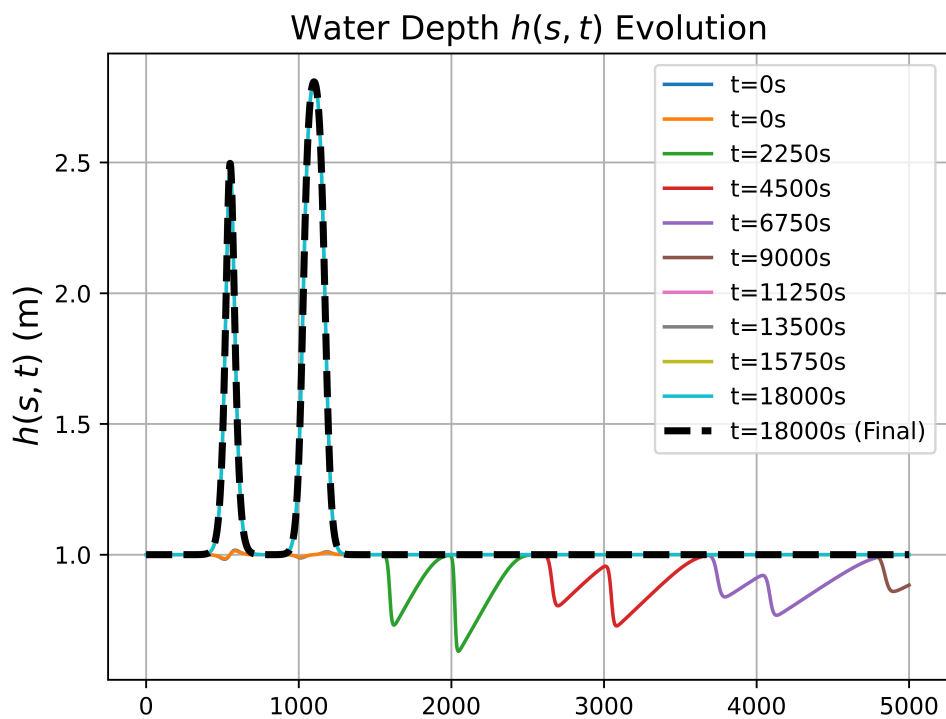


Figure 8: Height at different times

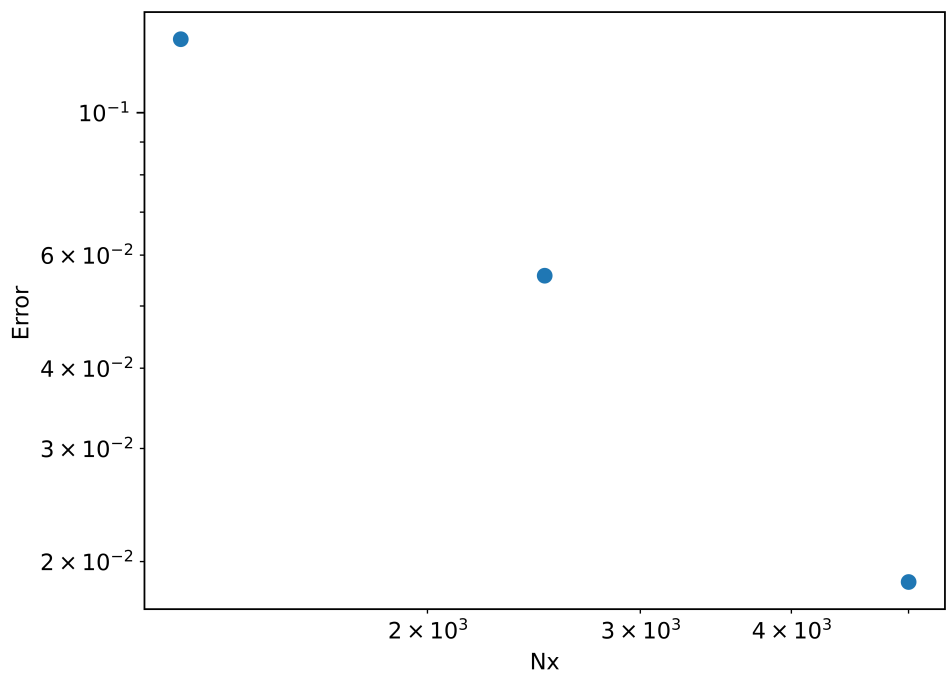


Figure 9: Error between finest grid ($N_x=10,000$) and coarser grids. Discharge at end of simulation was chosen and L2 norm calculated. CFL=0.5

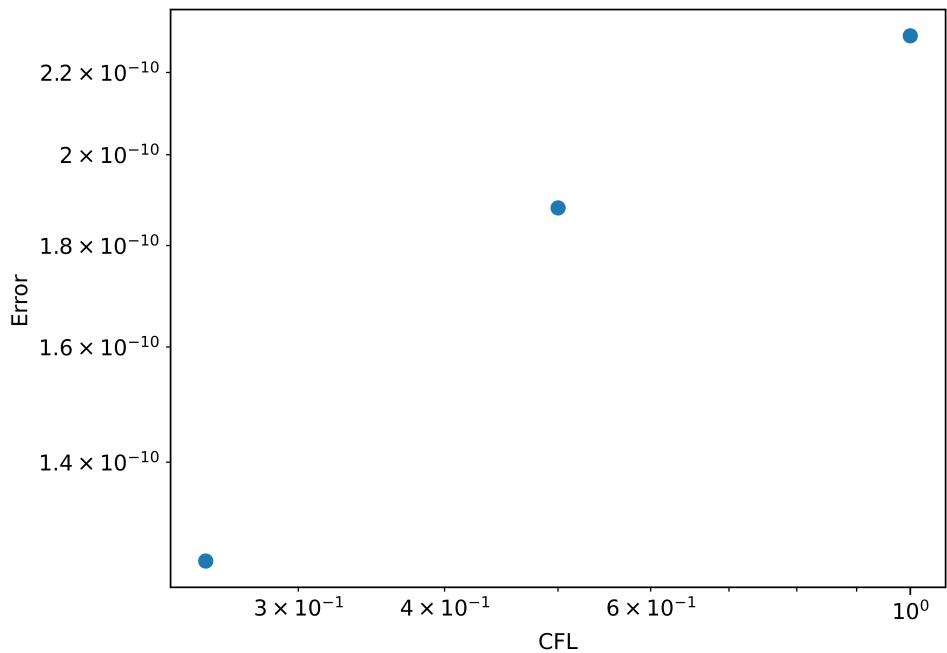


Figure 10: Error between simulation at smallest time step (CFL=0.125) and simulations with larger time steps. Discharge at end of the simulation was chosen and L2 norm calculated. N_x was constant at 2500.

1.6.2 Test Case 1

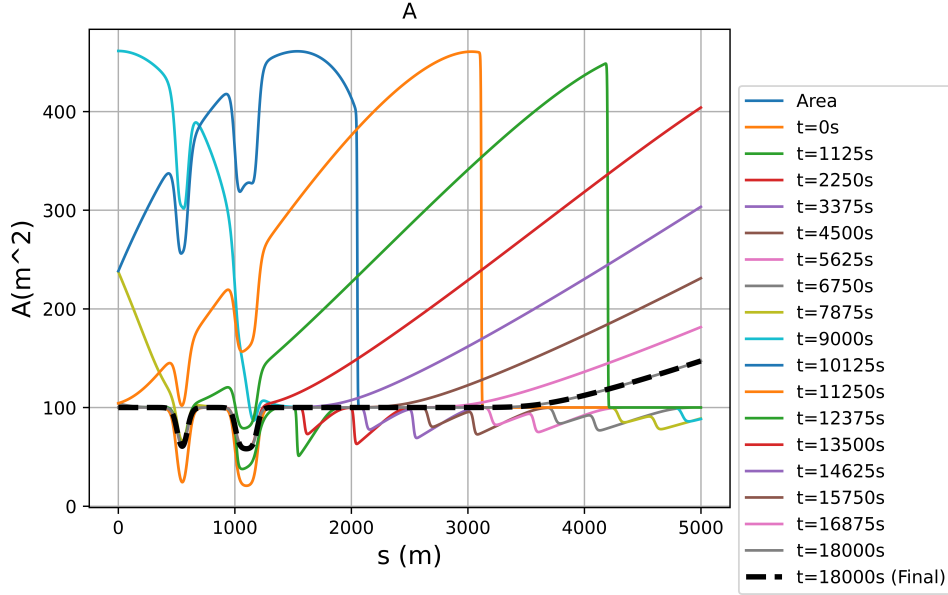


Figure 11: Area profile at different times.

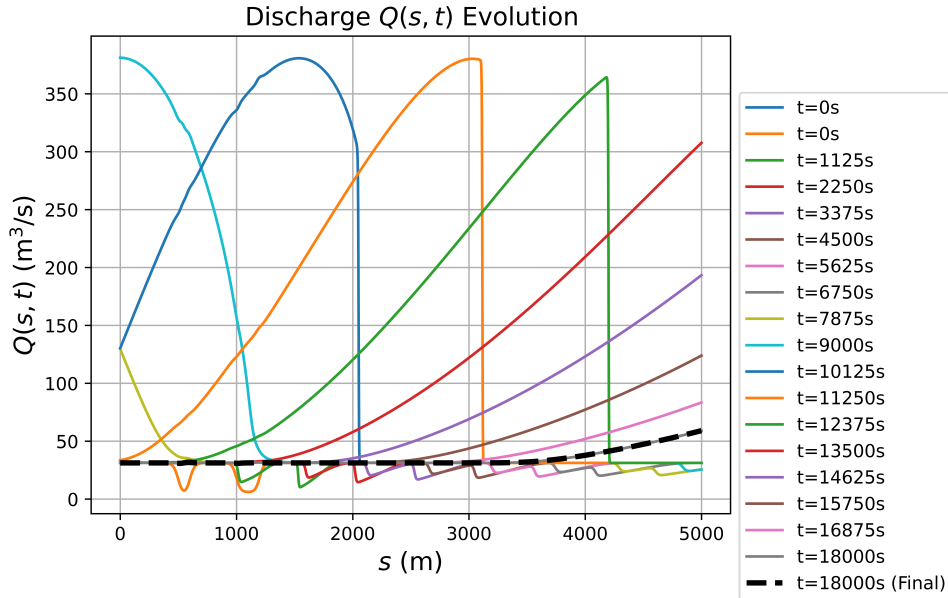


Figure 12: Flux profile at different times.

To find the numerical shock speed, the Area and Flux profiles were chosen between $t=12000$ and $t=13000$ since the profiles in these regions allow us to find the speed simply by tracking the position of the maximum value (Figures 14 and 15). The theoretical shock speed was found by using the Rankine-Hugoniot relation (see Figures 16 and 17). There is excellent agreement between the theoretical and numerical shock speeds (See table 1 and Figure 18). The spatial and temporal discretization is first order in both cases (Figures 19 and 20).

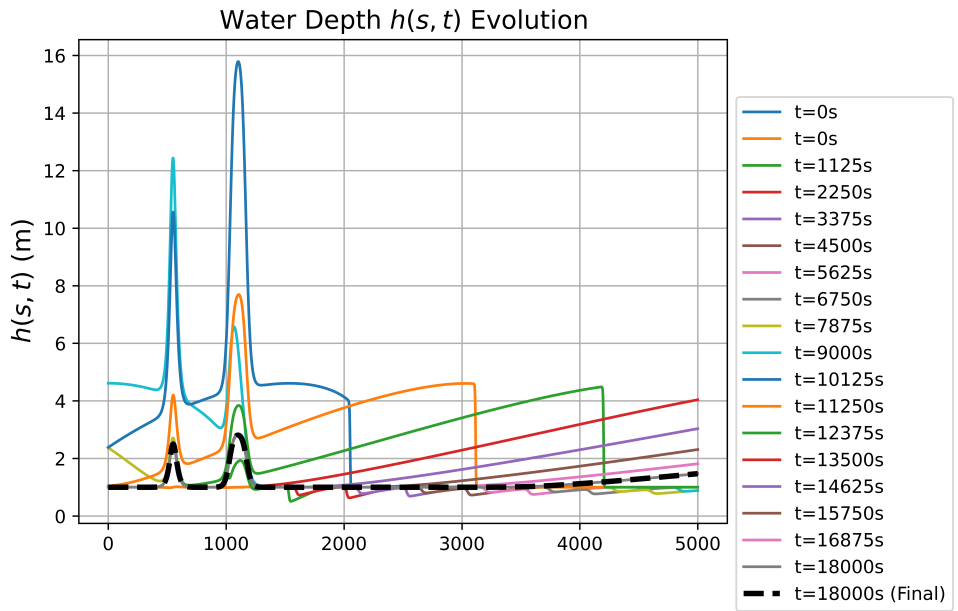


Figure 13: Height profile at different times.

Numerical Shock Speed	Theoretical Shock Speed	Time	% Error
0.958	0.960	12132	0.21
0.952	0.954	12451	0.21
0.946	0.946	12771	0

Table 1: Shock speed comparison

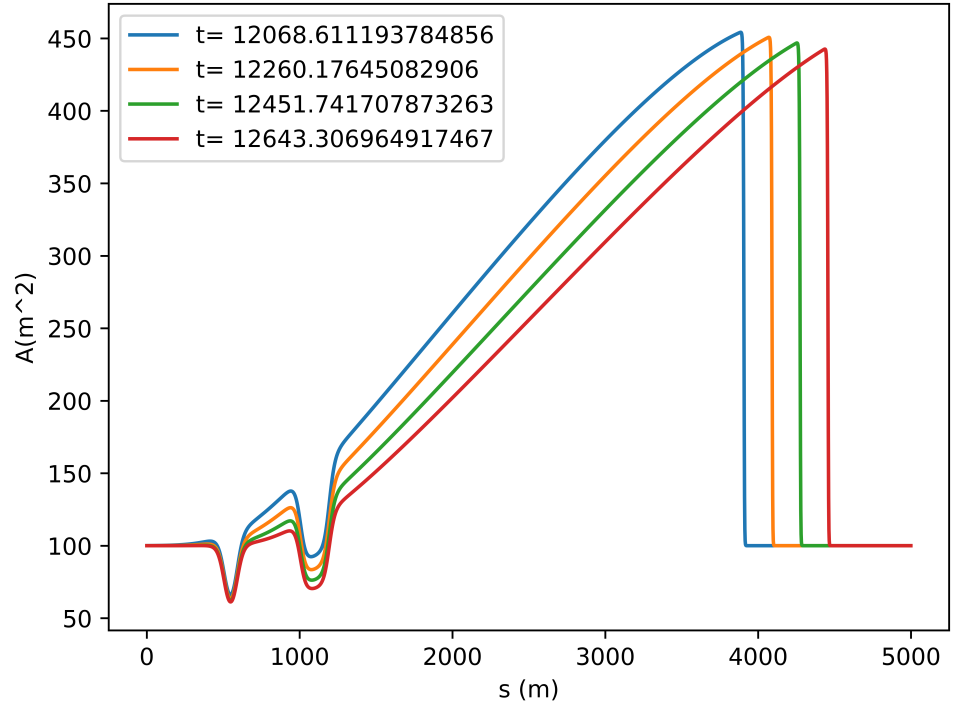


Figure 14: Area at different times

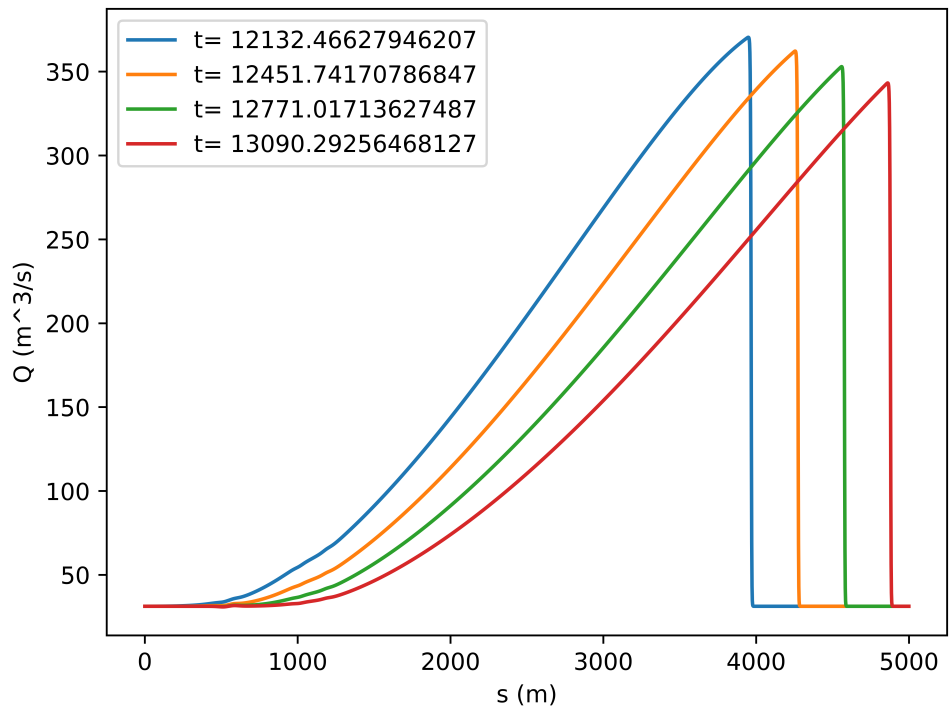


Figure 15: Flux at different times

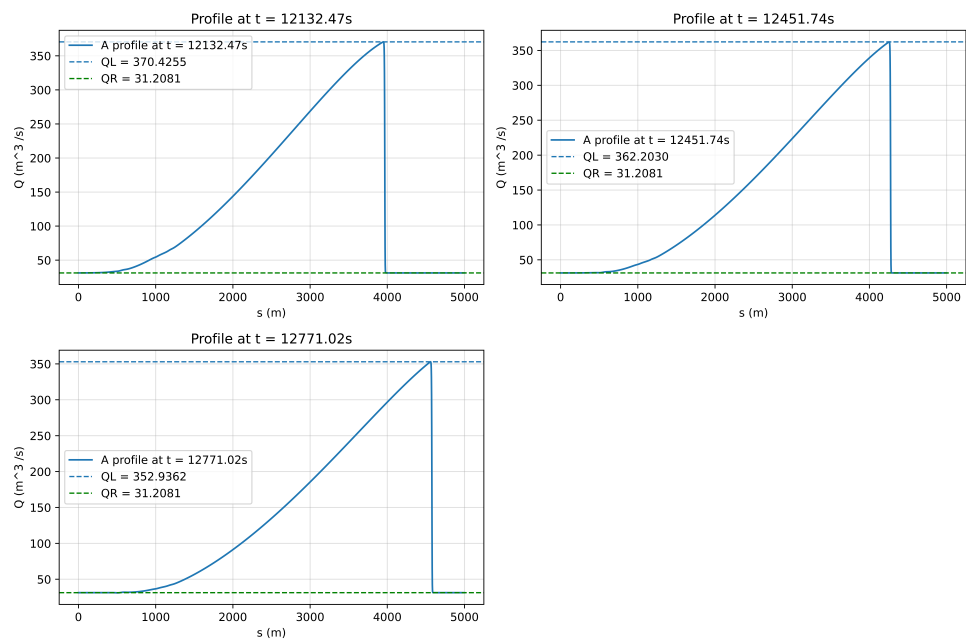


Figure 16: Flux profiles with AL and AR marked.

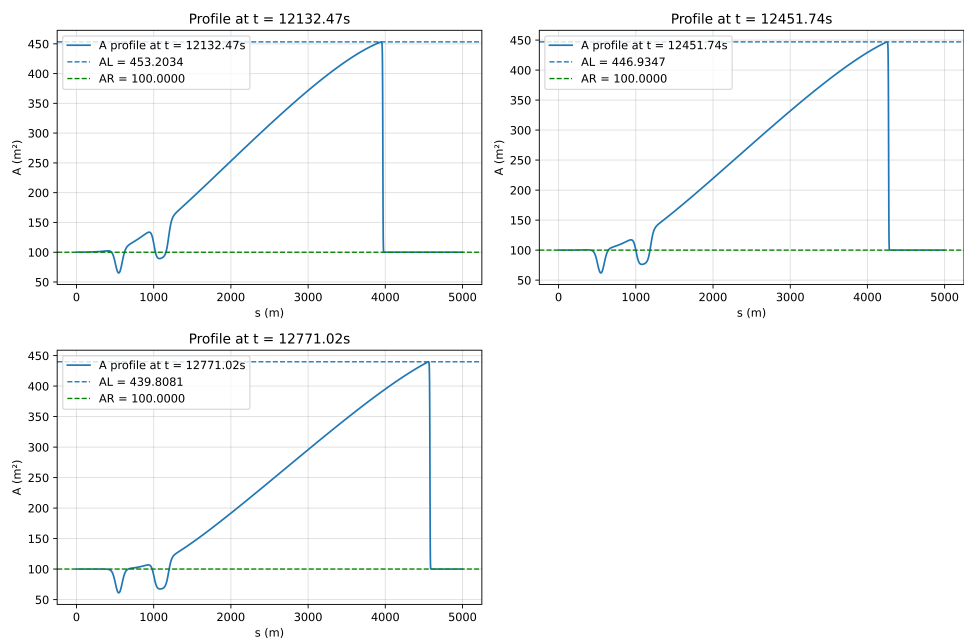


Figure 17: Area profiles with AL and Ar marked

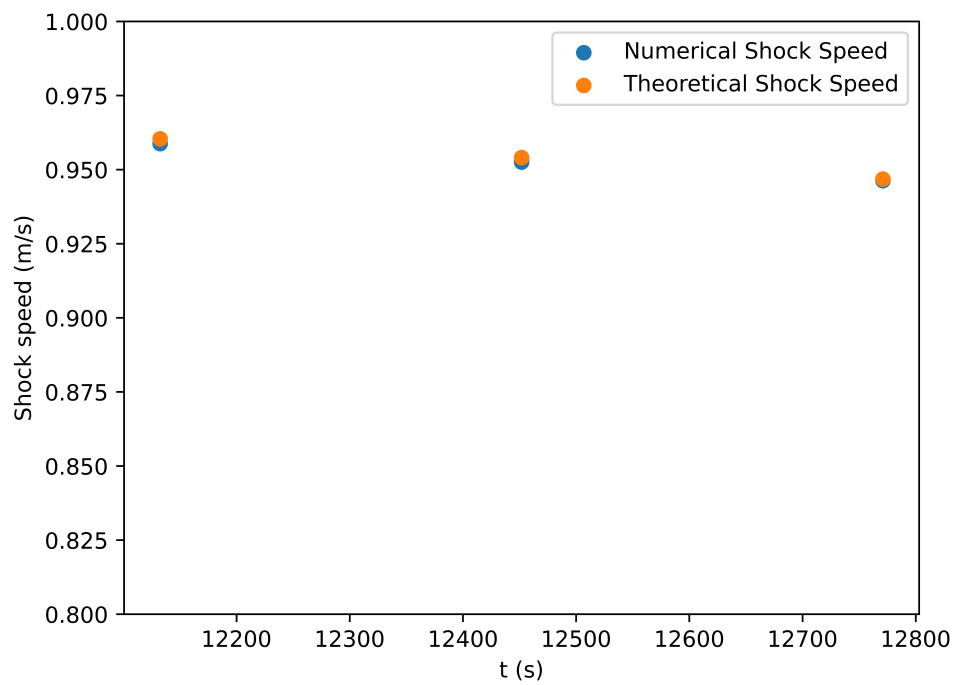


Figure 18: Shock speeds at different times

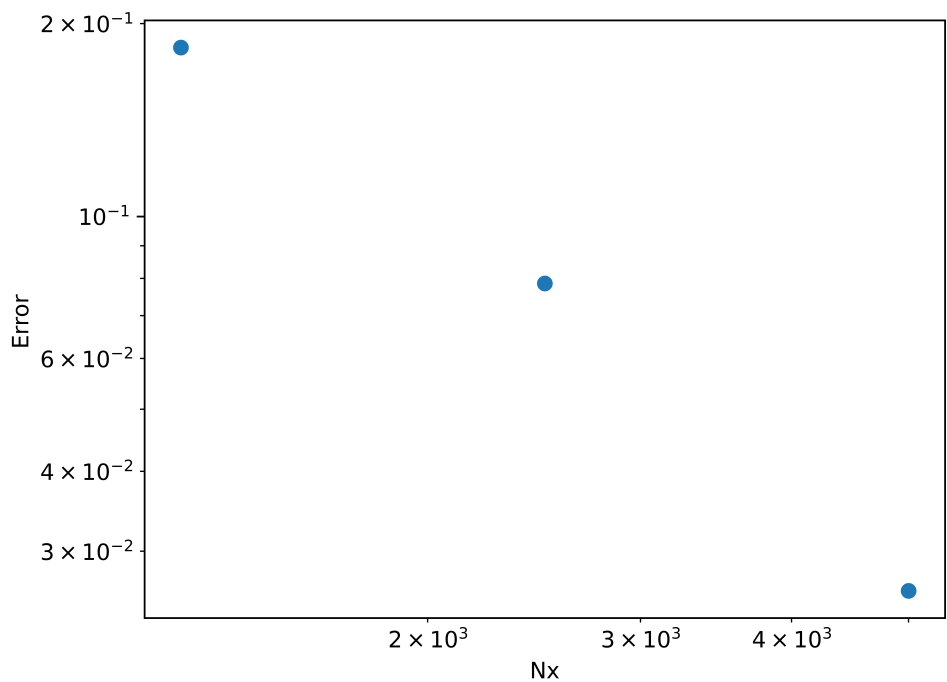


Figure 19: Spatial error. Flux at the end of the simulation was evaluated. L2 norm was used. CFL=0.5

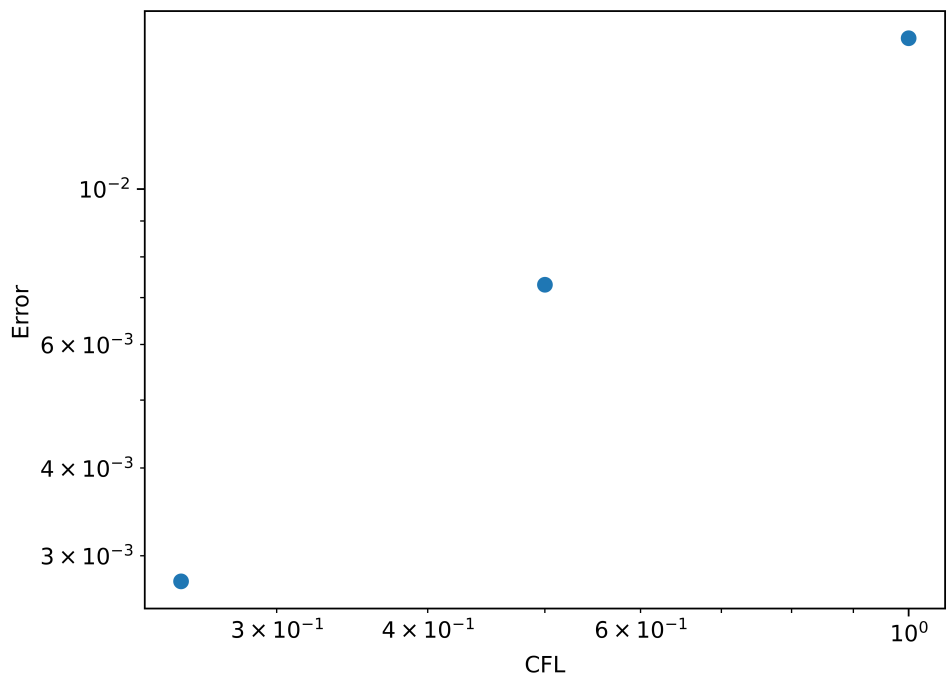


Figure 20: Temporal error. Flux at the end of the simulation was evaluated. L2 norm was used. $N_x = 2500$.

1.7 Testcase 2

1.7.1 Redo Testcase 0

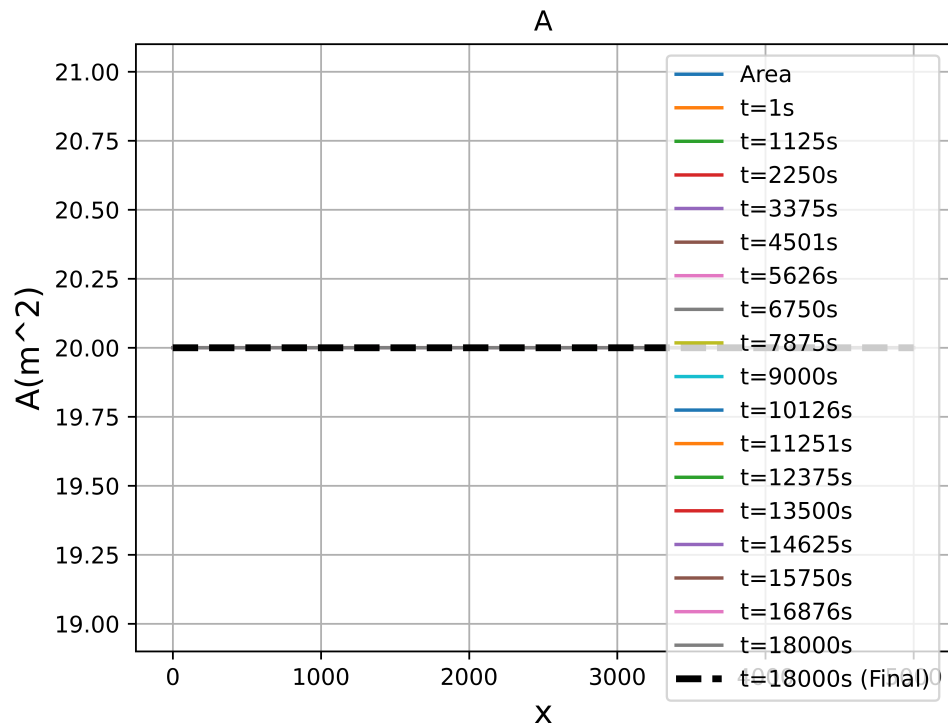


Figure 21: Area profile at different times with 0 flux.

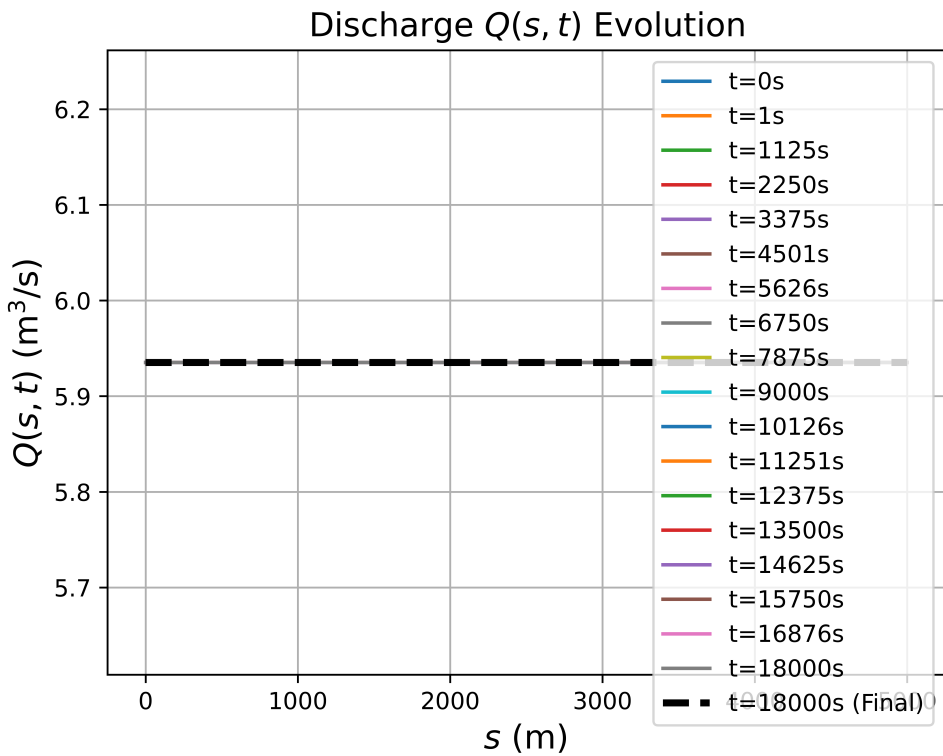


Figure 22: Flux profile at different times with 0 flux.

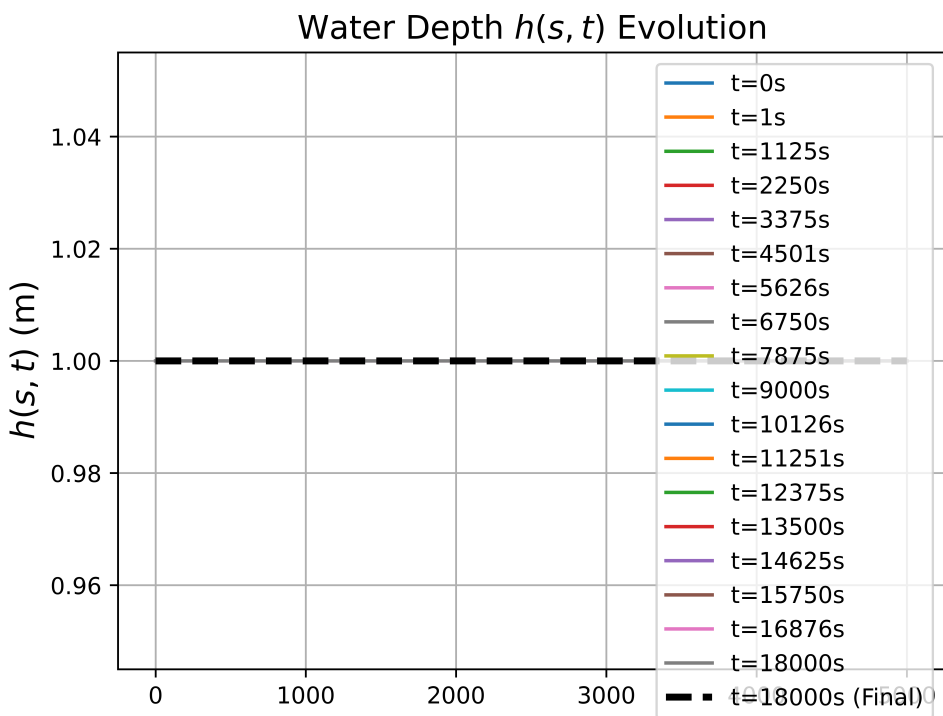


Figure 23: Depth profile at different times with 0 flux.

1.7.2 Redo of testcase 1

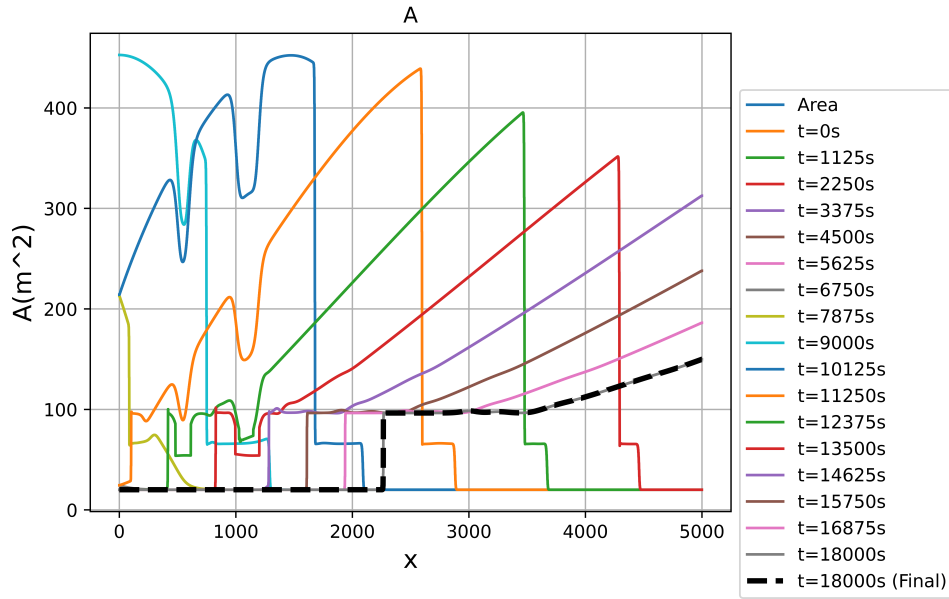


Figure 24: Area profile at different times.

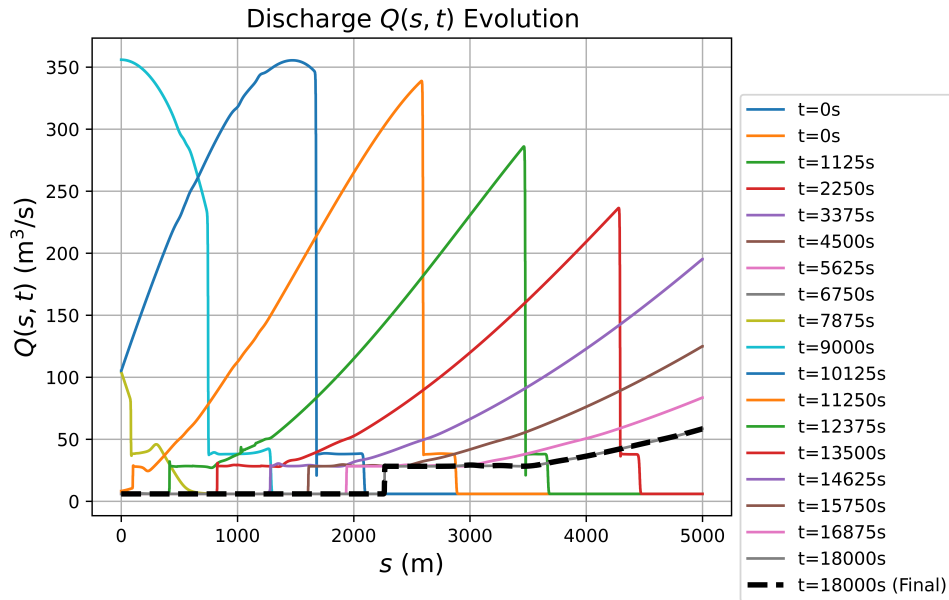


Figure 25: Flux profile at different times.

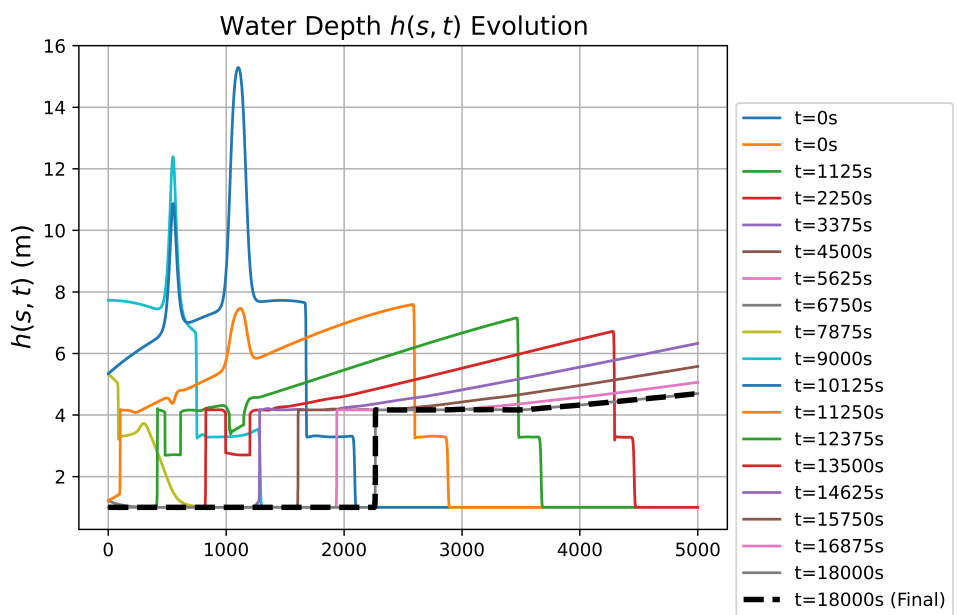


Figure 26: Flux profile at different times.

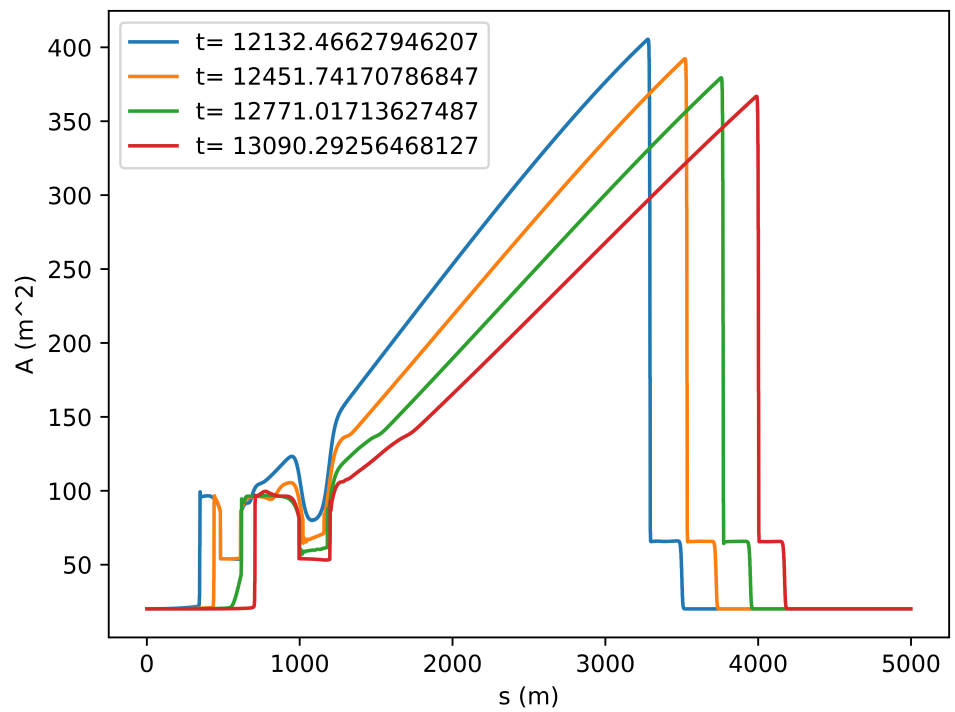


Figure 27: Area profile at different times. Times were selected to give well defined maxima.

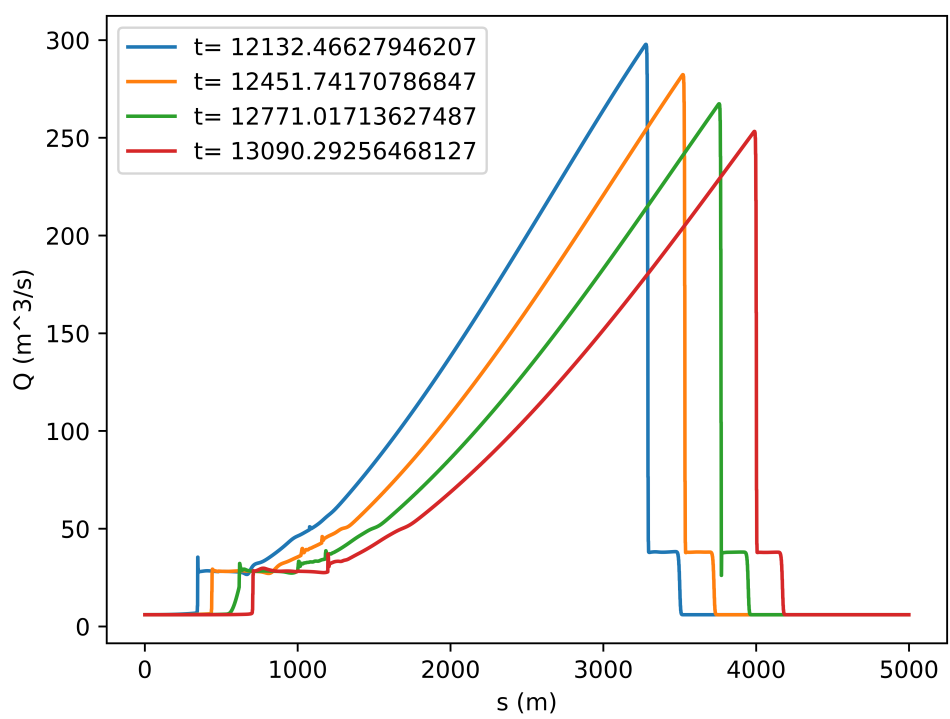


Figure 28: Fluxe profile at different times. Times were selected to give well defined maxima.

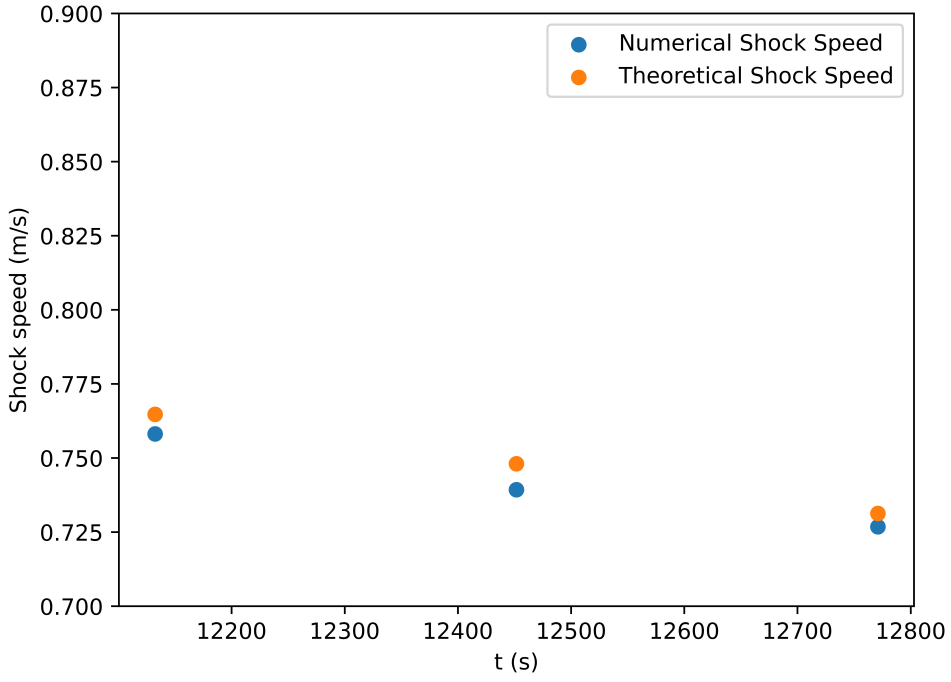


Figure 29: Numerical vs theoretical shock speed for test case 2

Numerical Shock Speed	Theoretical Shock Speed	Time	% Error
0.758	0.764	12132	0.79
0.739	0.748	12451	1.2
0.726	0.731	12771	0.68

Table 2: Shock speed comparison

The geometry gives a shock which is followed by a smaller shock, as shown in Figures 27 and 28, because the flow encounters two successive constrictions in the channel width that are close together. The theoretical shock speed and the numerical shock speed are very close, implying that the simulation is accurate (see Table 2 and Figure 29). As before, Figures 30 and 31, which show the temporal and spatial discretization error, demonstrate that the scheme is first order accurate in both space and time.

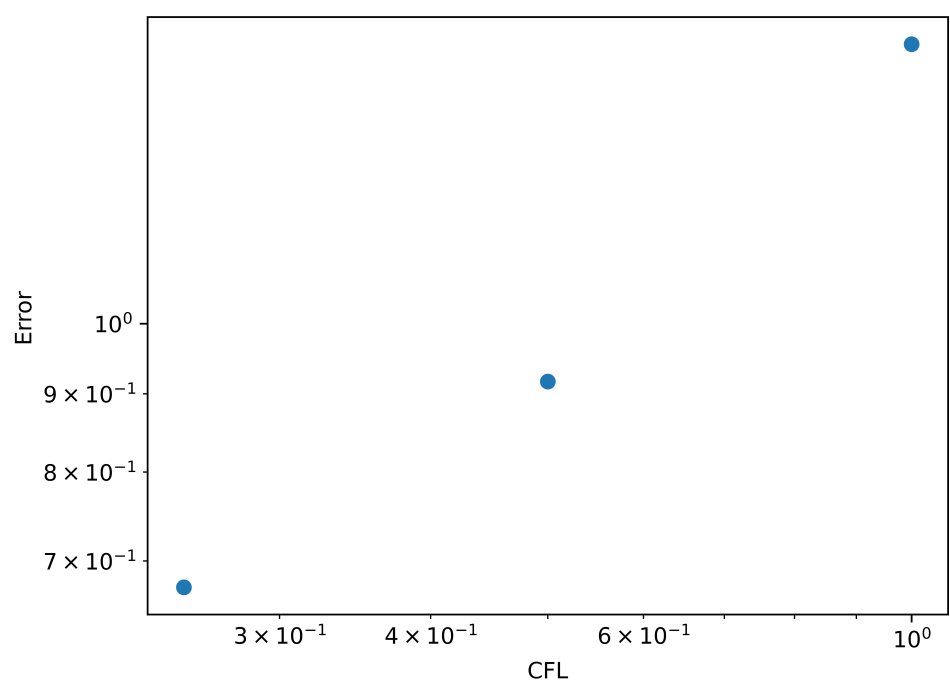


Figure 30: Time discretization errors. L2 norm was used. Nx=2500

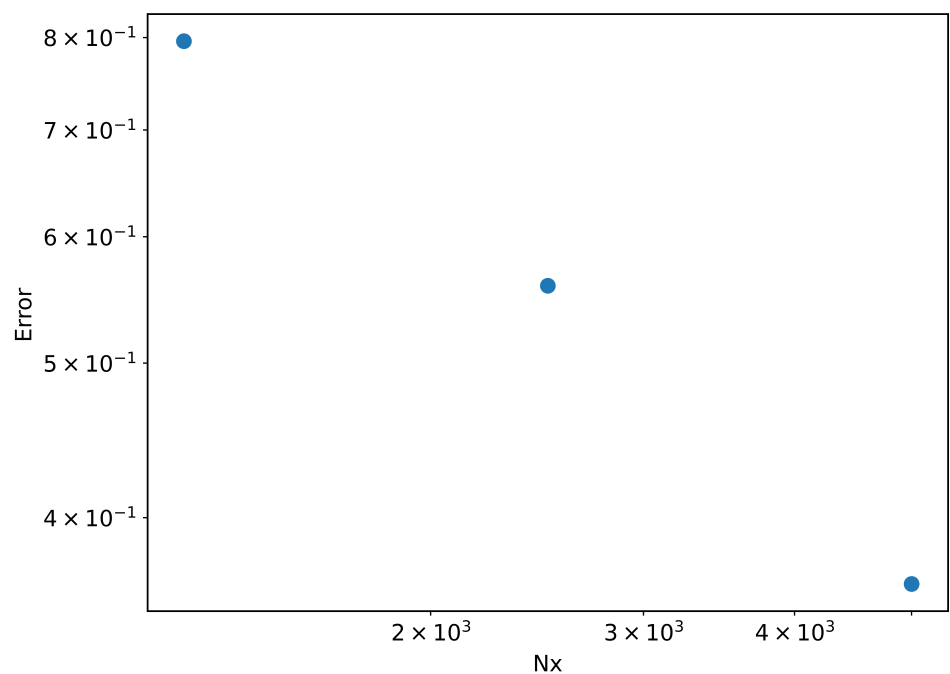


Figure 31: Spatial discretization errors. L2 norm was used. CFL=0.5

20/20 (nice)